Nonlinear finite element analysis of behaviors of steel beam–continuous compound spiral stirrups reinforced concrete…

Article *in* The Structural Design of Tall and Special Buildings · January 2012

DOI: 10.1002/tal.758

CITATIONS
3

READS
353

3 authors, including:

Wei Li
Wenzhou University
12 PUBLICATIONS **36** CITATIONS

SEE PROFILE

THE STRUCTURAL DESIGN OF TALL AND SPECIAL BUILDINGS
Struct. Design Tall Spec. Build. (2012)
Published online in Wiley Online Library (wileyonlinelibrary.com/journal/tal). DOI: 10.1002/tal.758

Nonlinear finite element analysis of behaviors of steel beam–continuous compound spiral stirrups reinforced concrete column frame structures

Wei Li[1]*,†, Qing-Ning Li[2] and Wei-Shan Jiang[2]

[1]*College of Architecture and Civil Engineering, Wenzhou University, Wenzhou, P.R. China*
[2]*School of Civil Engineering, Xi'an University of Architecture and Technology, Xi'an, P.R. China*

SUMMARY

Many tests and numerical research for RCS frame consisted of reinforced concrete (RC) column and steel (S) beam have been conducted in the USA and Japan over the past decades; they showed that the performance of the RCS system is superior to traditional concrete frame and steel frame. Up to the present, no research reports on composite CCSHRCS frame structure consisted of high-strength concrete columns confined with continuous compound spiral stirrups (CCSHRC) and steel (S) beam. Herein, an accurate finite element model of composite CCSHRCS frame is developed; the finite element model is investigated in order to fully include important factors such as local buckling of steel beam and nonlinear behavior of confined concrete; the validity of the proposed models is examined by comparing with the results of cyclic loading experiments on the RCS frame in reference. With the proposed model, the effect of composite CCSHRCS frame is discussed in detail. Copyright © 2012 John Wiley & Sons, Ltd.

Received 14 June 2011; Revised 17 October 2011; Accepted 18 November 2011

KEYWORDS: composite structures; finite element analysis; high-strength stirrups; RCS frame; failure model; load versus displacement

1. INTRODUCTION

It has been widely recognized that composite moment frames consisting of RC columns and steel (S) beams, or the so-called RCS system, can provide cost-effective alternative to traditional steel or RC construction in seismic regions. As opposed to conventional steel or RC moment frames, the problems associated with connections are greatly reduced, and the RCS frames are generally more economical than the purely steel or RC moment frames. The research program included extensive testing and finite element analyses of RCS beam-to-column connections and subassemblies, testing of reduced-scale and full-scale RCS moment frames and finite element analyses, seismic design studies and analyses of RCS moment frames, and development of guidelines and recommendations for detailed design work (Goel, 2004).

However, researches were rarely conducted on composite moment frames consisting of continuous compound spiral hoop reinforced concrete (CCSHRC) column and composite steel beam despite its potential benefits in construction speed and structural excellent ductility due to the use of CCSHRC column. Experimental research has been conducted that the CCSHRC column and CCSHRC–steel (S) composite connection, or the CCSHRC and steel (CCSHRCS) composite frames, which has the advantage of high-strength continuous compound spiral hoop confined high-strength concrete column, improves the strength and ductility and reduce the section size of the column, thereby increasing effective building space. As an 'undefined structural system', the composite CCSHRCS system cannot be easily adopted in design and construction practice. However, it has become recognized by more and more researchers and practicing professionals in recent years that structural systems that do not fully

*Correspondence to: Wei Li, College of Architecture and Civil Engineering, Wenzhou University, Chashan University Town, Wenzhou City, Zhejiang Province, 325035, P.R. China.
† E-mail: liweiwoaini521@yahoo.com.cn

satisfy the prescriptive requirements of current building codes can possibly provide satisfactory seismic performance. The desirable seismic characteristics must be validated by analysis and laboratory tests. However, because it is difficult from an economical viewpoint to conduct many experiments and due to the unique features of the tested specimens and material heterogeneity, it was also difficult to understand the complex seismic behavior of beam–column connections and framed structures. Furthermore, the effect of several influencing parameters such as plate thickness, axial load and the effect of confining cannot be varied in a limited number of experiments. In order to quantify and decide the influence of critical design parameters, it is necessary to propose a robust numerical model. Following this understanding, a series of finite element analysis for composite structures were conducted by many researchers.

Liu and Foster (1998) developed a finite element model to investigate the response of concentrically loaded columns with concrete strength up to 100 MPa. The model was based on the explicit microplane model of Carol *et al*. (1992); the numerical results were shown that for confined high-strength concrete columns, the tie steel is not at yield at the peak load and that tension stains at the cover-core interface of high-strength concrete columns are large enough to account for early cover spalling that has been observed experimentally.

Yu *et al*. (2010a) presented a modified Drucker–Prager (D–P) type model and implemented it into ABAQUS. Comparisons of numerical predictions obtained using this modified (D–P) type model and test results have demonstrated the capability of the proposed model in providing close predictions of the behavior of both actively confined and fiber reinforced polymer-confined concrete. Hajjar *et al*. (1998) proposed a 3D modeling of interior beam-to-column composite connections with angles by means of the ABAQUS code (2006).

Salvatore *et al*. (2005) studied seismic performance of exterior and interior partial-strength composite beam-to-column joints by using the ABAQUS software.

Hu *et al*. (2003) proposed proper material constitutive models for concrete-filled tube columns, and they were verified by the nonlinear finite element program ABAQUS against experimental data. The stress–strain curve of the reinforcing tie is assumed to be elastic–perfectly plastic. In the analysis, the Poisson's ratio v_s and the elastic modulus E_S of the steel tube are assumed to be $v_s = 0.3$ and $E_S = 200$ GPa.

Zhao and Li (2008) studied the nonlinear mechanical behavior and failure process of a bonded steel–concrete composite beam by using finite element program ABAQUS. It can be seen that the numerical results and experimental data match very well.

Bursi *et al*. (2005) studied the seismic performance of moment-resisting frames consisting of steel–concrete composite beams with full and partial shear connection by using ABAQUS program. The results have demonstrated the adequacy of three-dimensional finite element models based on the smeared crack approach.

Han *et al*. (2008) presented a finite element modeling of composite frame with concrete-filled square hollow section columns to steel beam; the finite element program ABAQUS was adopted and it is shown that the finite element modeling was able to reasonably predict the lateral load versus lateral displacement relationship of composite frame and the ultimate lateral load carrying capacity.

Wu *et al*. (2009) studied the effect of wing plates numerically by simulating H-beams in bolted beam–column connections as cantilever beams using ABAQUS; the simulation agrees well with the experimental results.

Set against this background, this paper will apply the finite element program ABAQUS to simulate the seismic behavior of the CCSHRCS composite frames, i.e. first to develop a nonlinear three-dimensional finite element model of a previously tested RCS frame specimen by using ABAQUS program and calibrate a nonlinear finite element model and further use it to investigate the seismic behavior of a composite CCSHRCS frame.

2. FINITE ELEMENT MODEL

2.1. General descriptions

In order to accurately simulate the actual behavior of the RCS frame specimen, the main six components of the frames need to be modeled. These are the confined concrete columns, the interface and

DOI: 10.1002/tal

contact between the concrete in joint regions and the structural steel (e.g. band plates, cover plates), the interface and contact between the shear connections of the steel beam and the concrete slab, the interaction of reinforcement and concrete, the connection details between the RC columns to the steel beam, and the steel beam, the simulation procedure for connection. In addition to these parameters, the choice of the element type, mesh size, boundary conditions and load applications that provide accurate and reasonable results is also important in simulating the behavior of structural frames.

2.2. Material modeling of concrete

In the conventional concrete models, the behavior under compressive stresses is usually represented by the plasticity model, while the behavior under tensile stresses is expressed by the smeared cracking model. The smeared cracking model, however, often encounters numerical difficulty in the analysis under cyclic loading. To circumvent this situation, the concrete damaged plasticity model implemented in ABAQUS (2006) is used herein. By experimental observations on most of quasi-brittle materials, including concrete, when the load changes from tension to compression, compression stiffness recovers with the closure of crack. In addition, when the load changes from tension to compression, once the crushed micro-cracks occur, the stiffness in tension will not be restored. This performance corresponds to the default values $w_t = 0$ and $w_c = 1$ in ABAQUS, where w_t and w_c are respectively the weight factor for tensile and compressive stiffness restoration under cyclic loading. Figure 1 describes the default properties under uniaxial cyclic loading.

2.3. Material modeling of reinforcement

In this paper, in order to simplify the problem in the analysis of finite element method, it is assumed that the stirrups and longitudinal reinforcements in the concrete columns are ideal elasto-plastic material, regardless of the reinforcement service stage and Bauschinger effect in their stress–strain relations, i.e. before the steel yields, the stress–strain curve is a leaning line, and after that, it should be simplified to a horizontal line, as shown in Figure 2.

2.4. Material modeling of structural steel

There are a variety of constitutive models used to describe the mechanical properties of structural steel, e.g. the ideal elasto-plastic model, the isotropic strengthening model and the stochastic strengthening model. The von Mises yield criterion with bilinear model is adopted in this study.

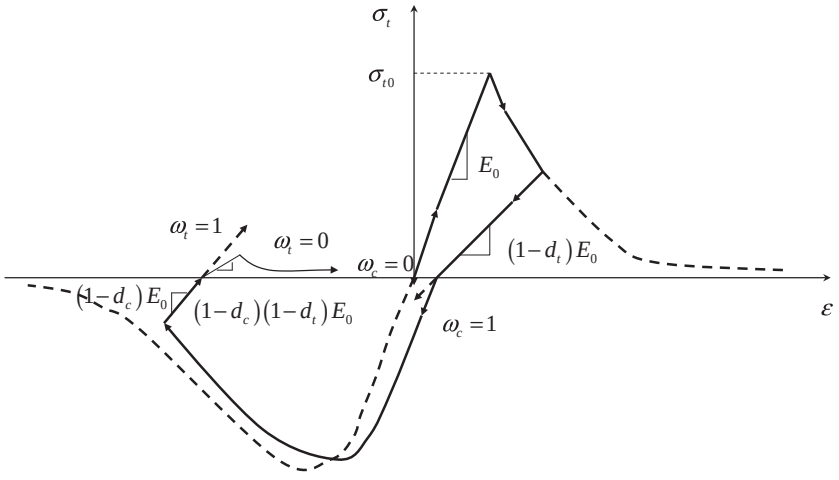

Figure 1. Uniaxial load cycle (tension–compression–tension) assuming default values for the stiffness recovery factors: $w_t = 0$ and $w_c = 1$.

DOI: 10.1002/tal

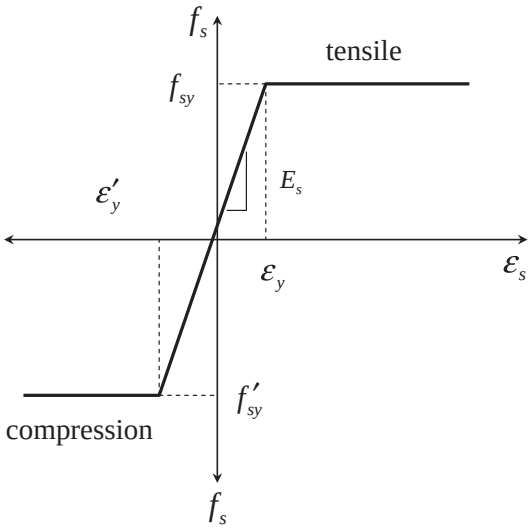

Figure 2. Stress–strain relationship of reinforcement.

2.5. *Interactive modeling between concrete and reinforcement, concrete and structural steel*

Since the joints of the steel beam and the concrete column connect together by welding a face bearing plate at the steel beam flange in the frame structure, the beam–column and face bearing plate are well confined with the joint regions to make the joint regions slip a little. Tests have shown that concrete and steel in the joint regions can still work together until the destruction of the beam–column joint. Salvatore *et al.* (2005) studied the seismic performance of exterior and interior partial-strength composite beam-to-column joints by using the ABAQUS software; a hardening elasto-plastic material was modeled by using discrete two-noded beam elements, and dimensionless bond-link elements were adopted to connect the concrete and steel nodes, but friction between the steel bars and the concrete slab was not modeled because it has a little influence on substructure responses. On the other hand, in the joint adding bonding element, the analysis will become very complicated, so the bond slip of the joint regions was not considered. In this paper, 'Interaction' module 'Constraint' command in ABAQUS is taken as Embedded region embedded in the reinforced concrete columns. In this condition, there is no relative slip between the steel and the concrete. Steel beam and concrete column, face bearing plate and concrete in joint regions are directly constrained by module 'Tie' command in the 'Interaction' to make a binding constraint, so there is no relative slip between them.

2.6. *Bounding conditions and loading*

The boundary conditions and loading manners of RCS frame structures are specific in this paper: the connection construction of the steel beam–concrete column is shown in Figure 3(a). The concrete column foot is fixed constraint, the axial load is imposed by the loading plate on top of the column, and the horizontal load is imposed on the beam. In the ABAQUS software, the boundary conditions are set as follows: three concrete columns with fixed boundary constraints and the 'Merge' command of 'Assembly' module are used to merge the steel beam and the face bearing plates. In this case, the steel beams and the face bearing plate can be regarded as fixed constraints. The loading plate and the interface of the column cap are constrained by the 'Interaction' module 'Tie' command.

The loading of the frame is divided into two categories, the axial load at the top of the framed column and the horizontal load at the end of framed beam, so two load steps are required in the ABAQUS code. The specific methods are as follows: the axial load is applied at the top of the three framed columns, respectively; first, it is applied to the interior column and then to the other two exterior columns and set it as a load step; when axial loading is completed, the horizontal load should be loaded at both ends of the framed beam, and displacement loading is adopted in order to obtain the load–displacement curves of the frame, i.e. displacement is applied at the end of the beam (applied

DOI: 10.1002/tal

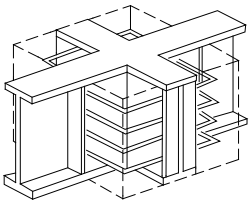

(a) The connection construction

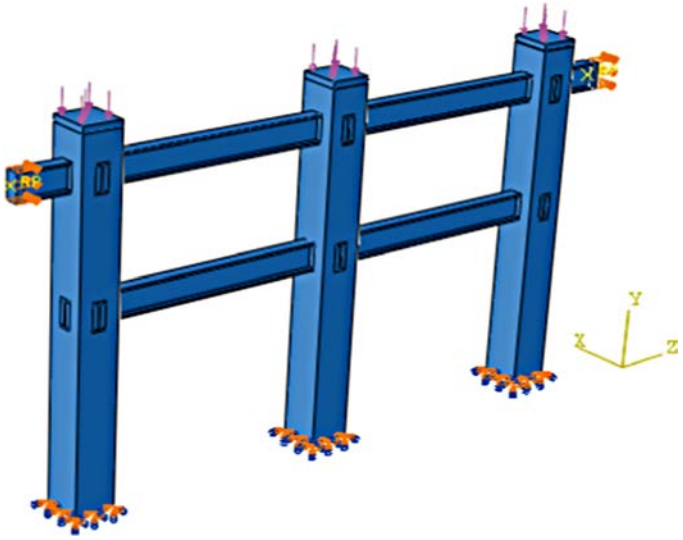

(b) Load modeling of a composite RCS frame

Figure 3. The connection construction and load modeling of a composite RCS frame. (a) The connection construction and (b) load modeling of a composite RCS frame.

displacement boundary conditions that have been known). In order to avoid stress concentration, the 'Load' module 'Pressure' of ABAQUS is adopted for the axial load. Figure 3(b) is the loading model diagram of the composite RCS frame.

2.7. The selection of element type and meshing

In order to simulate detail characteristics of the steel beam–concrete column joint areas, a three-dimensional solid element with reduced integration eight-node formulation (C3D8R) are adopted for steel beams and concrete. Compared with the high-order isoparametric element, although the accuracy of this element is slightly lower, it can reduce much freedom degree, which can greatly reduce the computational cost. Two-node linear three-dimensional truss element (T3D2) is used to understand the force characteristics of the stirrups and longitudinal reinforcements in the concrete columns.

Figure 4 shows the cross-section mesh diagram of the finite element model on the concrete columns, steel, steel beams and the whole face bearing plate, and the beam–column joint region in this paper. Because of the complexity of the beam–column joint regions, in order to ensure the accuracy of the results, it is subdivided.

3. VALIDITY OF FINITE ELEMENT MODELING

In order to validate the finite element model developed in this paper, the numerical results and the test results in the literature (Iizuka *et al*., 1997; Li *et al*., 2011) are compared with. The detail sizing and

DOI: 10.1002/tal

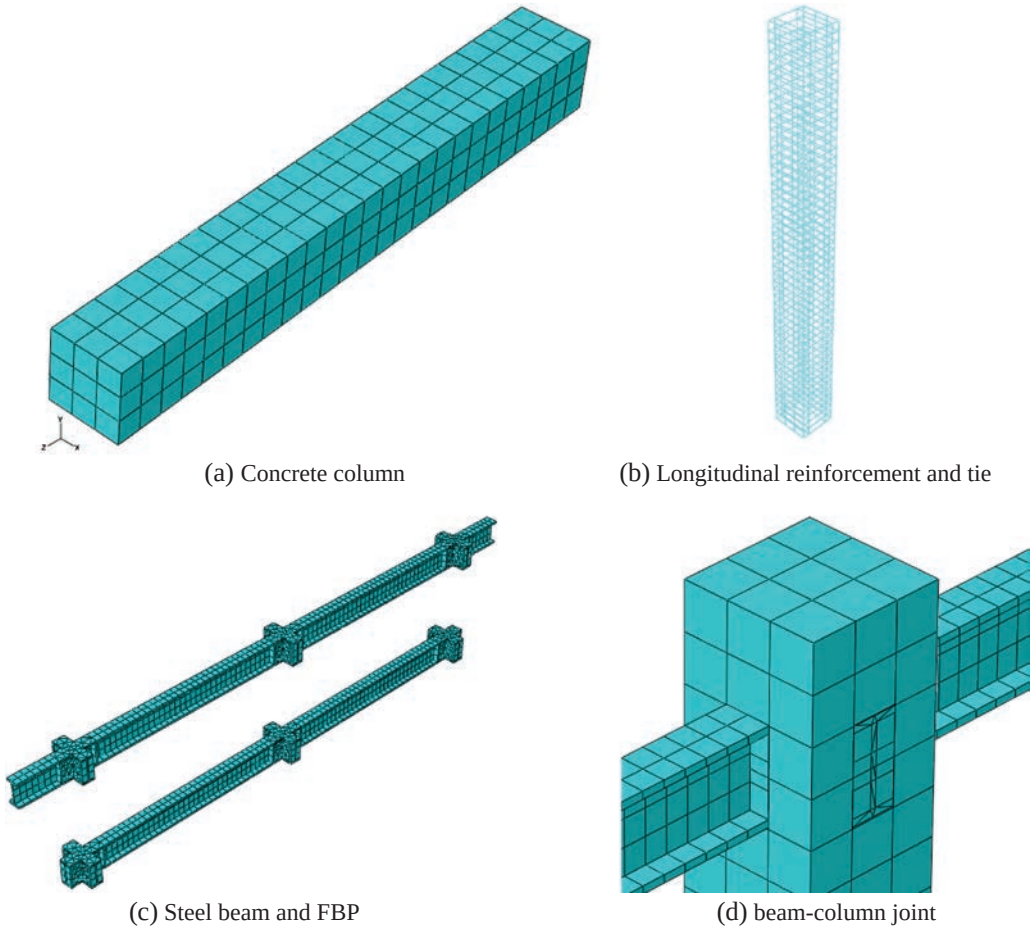

(a) Concrete column (b) Longitudinal reinforcement and tie

(c) Steel beam and FBP (d) beam-column joint

Figure 4. Meshing sketch of section. (a) Concrete column, (b) longitudinal reinforcement and tie, (c) steel beam and face bearing plate and (d) beam–column joint.

reinforcement are shown in Figure 5. Details of specimens are seen in Table 1, and the corresponding material properties are shown in Table 2.

In accordance with the specific parameters of the mentioned specimens, a finite element model of the specimen is developed by ABAQUS, as is shown in Figure 6. The frame specimen model consists of 18 511 elements, 17 566 C3D8R solid elements and 945 T3D2 truss element. Since the beam–column joint region is under a larger force, in order to avoid distortions in the joint area, first, complex geometric models of the joint regions are cut into simple geometric models, and further element joints are subdivided by geographical mesh.

3.1. The load–displacement relation for the composite RCS frame

The relationship of the load–displacement for the RCS framed specimen is obtained by calculation, and it is shown in Figure 7. At the initial load for the frame, when horizontal displacement is within 20 mm, the structure has not yet reached the ultimate bearing capacity (when a steel beam or column reaches yield, the framed specimen is under the ultimate load), and the load–displacement curve has a nearly linear relationship. When the horizontal displacement is more than 20 mm, with the increase of displacement for the load–displacement curve, the load slowly increases until yielding to the destruction of the structure. In this condition, the horizontal ultimate load and displacement are respectively 797 kN and 77.8 mm. In addition, when the test procedures are adjusted, ANSYS software (ANSYS, Inc., Canonsburg, PA, USA) is used for analysis on load–displacement relationship for framed specimens, and the comparison with the calculation by ABAQUS is shown in Figure 8. The

DOI: 10.1002/tal

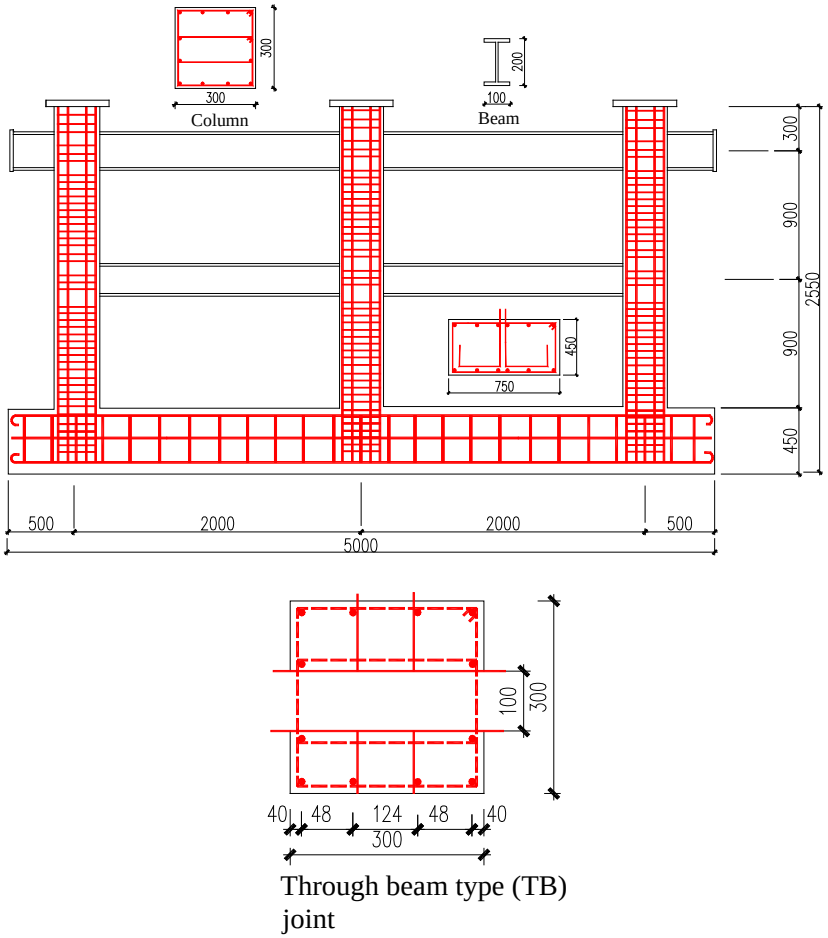

Figure 5. Specimens tested by Iizuka *et al*. (1997).

Table 1. Details and size of specimen.

Detailed parameters of the specimen		
Column	Section	B × D = 300 mm × 300 mm
	Longitudinal reinforcement	12-D19 ($\rho_t = 1.28\%$)
	Tie	4D-10@50 ($\rho_w = 1.9\%$)
	Axial load	(Exterior column) 0.1BD $\sigma_B = 242\,100$ N
		(interior column) 0.2BD $\sigma_B = 484\,200$ N $\sigma_B = 26.9$ N/mm^2
Beam	Section	BH-200 × 100 × 12 × 16 (mm)
Beam–column joints	Tie	4D-6@50 ($\rho_w = 0.85\%$)

load–displacement curve calculated by ANSYS in Figure 8 does not descend obviously, and the load is more than 700 kN, when displacement is 15 mm. However, the ultimate load and displacement are 1021 kN and 47.6 mm, respectively, and they are visibly higher than the calculated values by ABAQUS. The load–displacement curve calculated by ABAQUS is compared with the experimental results and is shown in Figure 8. The calculated results by ABAQUS agree well with the experimental value, while the calculated values by ANSYS are obviously higher than the experimental value because the crushing and the stiffness degradation of concrete under compression of concrete constitutive model in the ANSYS program were not considered, resulting in the calculated values higher than the actual value. Table 3 shows the comparison between the relation of horizontal load–displacement and the value calculated by ABAQUS. From that, the calculated values are in good agreement with the experimental values; it indicates that the ABAQUS software can simulate the load–displacement relations of this

DOI: 10.1002/tal

Table 2. The properties of materials.

Specimen		Compression strength (N/mm^2)	Tensile strength (N/mm^2)	Modulus of elasticity ($10^4 N/mm^2$)
Column		26.9	1.91	2.21
Foundation		29.4	2.62	2.19
Specimen		Yield strength (N/mm^2)	Tensile strength (N/mm^2)	Modulus of elasticity ($10^5 N/mm^2$)
Steel Reinforcement	D6	386	543.5	1.79
	D10	375.3	516.3	1.69
	D19	385.4	556	1.77
Steel plate	12 mm	312.4	463.9	1.97
	16 mm	299.8	425.4	1.95

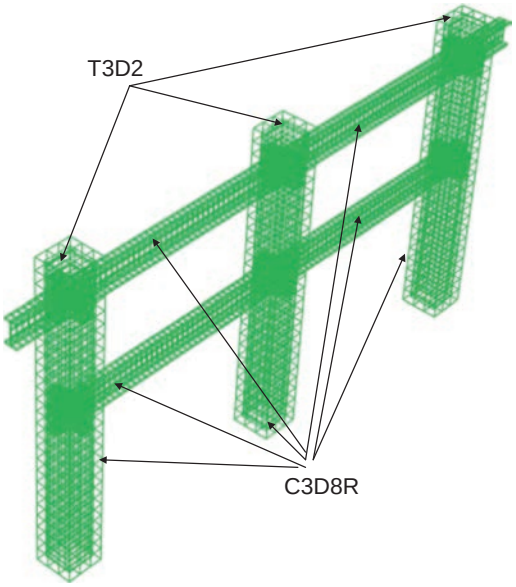

Figure 6. Finite element model of framed specimen.

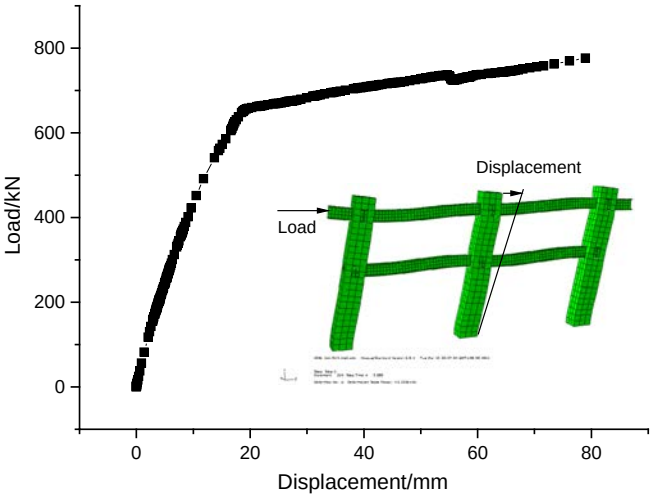

Figure 7. Relationship of load–displacement of framed specimen based on finite element method.

DOI: 10.1002/tal

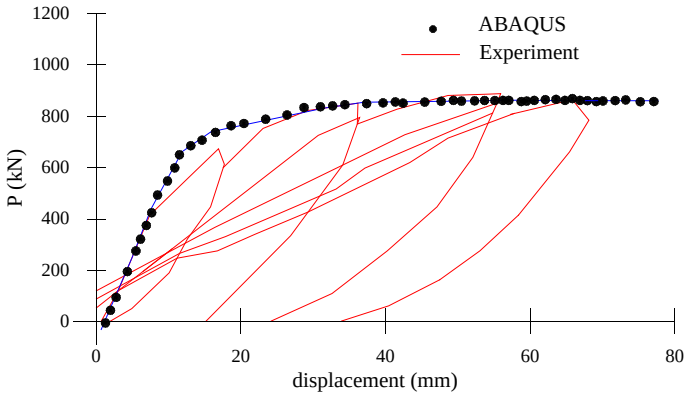

Figure 8. ABAQUS and ANSYS versus experimental relationship of load–displacement of framed specimen.

Table 3. Load drift based on calculated and experimental results.

		Experimental results	Calculated results	Calculated/ experimental
	Load (kN)	Interior column	Interior column	
Location of yield	Column foot at the	639	658.015	1.030
	first story	1/113	1/114.17	0.990
	Column cap at the	787	776.45	0.986
	second story	1/25	1/28.50	0.877
	Steel beam at the	885	797	0.901
	second story	1/33	1/30.64	1.078

composite frame. However, it should be noted that the horizontal load–displacement curve in the model is influenced not only by the constitutive relation of concrete materials but also by the constitutive relation of different materials. If the choice of constitutive model of materials is inappropriate, it will result in larger deviation of the calculated results, or it will lead to serious distortion of calculated results. Therefore, when the numerical model is used, the setting of each parameter should be grasped to make the model reflect the actual situation. It is also necessary to master the computational efficiency of the comprehensive computer.

3.2. The failure model for composite RCS frame

The composite RCS frame is under axial and horizontal load; with the horizontal load increasing, the moments of the beam and column ends will correspondingly increase. When the moment values of the column and beam ends reach to the ultimate flexural capacity of the section, plastic hinge will appear in the corresponding position. The force diagram of the RCS composite frame is shown in Figure 9. In

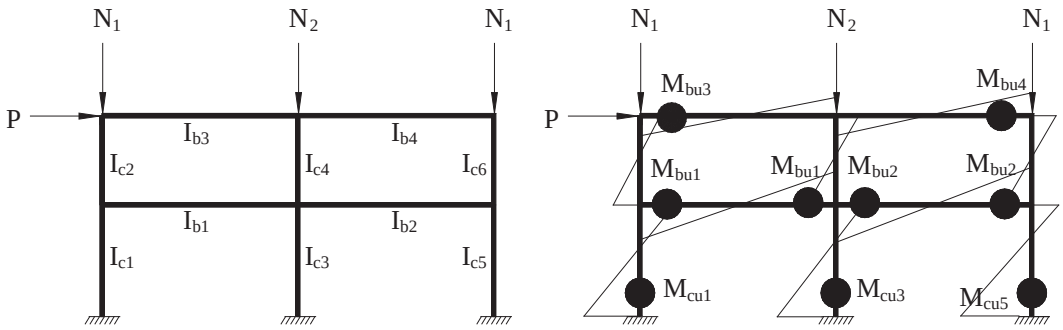

Figure 9. The moment of RCS composite frame under lateral load.

DOI: 10.1002/tal

the elastic stage, according to the calculation methods of structural mechanics, the axial force N of the framed column has no impact on the first-order moment, but the axial load N will have an impact on the moment when the second-order effects are considered. Meanwhile, because of the presence of the axial load for the framed columns, the framed column is a typical flexural component at this time. The axial load will generate additional lateral force to the framed column; it means that increasing the moment of the column end will reduce the ultimate flexural capacity of its cross section.

Therefore, only the frame is designed to meet the requirement of 'strong column and weak beam' and 'strong joint and weak component'. The RCS frame may always show yield mechanism that the plastic hinges first occur at the end of the beam. Figure 10 shows the yield and destruction process for the calculated RCS framed specimens, (1) the shear yield for beam web near the interior column joints of the second floor, (2) the flexural yield at both sides of steel beam flanges at the top of exterior column joints, (3) the shear yield for at both ends of the steel beam web near the exterior column joints of the second floor, (4) the tension and compression yield for longitudinal reinforcements of the foot of the interior column, (5) the tension and compression yield for longitudinal reinforcements of the foot of the exterior column, and they are compared with the test results. Calculation results generally agree with the experimental results, and the experimental result is that three column feet yield in turn, respectively. This is because the axial loads at the top of the column in the test will change as the horizontal load increases. In theory, the axial load is constant, but as the horizontal load increases, the column deformation will occur; at this time, the axial force at the top of the column will decrease, in the test, in order to compensate for the loss of axial load in that the axial load will continue to be applied on the columns, thus increasing the axial load at the top of the column artificially, thereby increasing the moment of the column end. So yield occurred so early for the longitudinal reinforcements at the bottom of the column. For the numerical calculation, the axial load applied to the top of the column can be kept constant. Overall, in the calculated and experimental results, the plastic hinges generally first occur in the beam end near the joint region and then yield occurs in the longitudinal reinforcements of the foot of the column.

4. NONLINEAR FINITE ELEMENT ANALYSIS OF COMPOSITE CCSHRCS FRAME

4.1. General descriptions

The ABAQUS software has been used in the previous section to analyze the performance of composite RCS frame, and the model is validated by the test results in the literature. The previous finite element

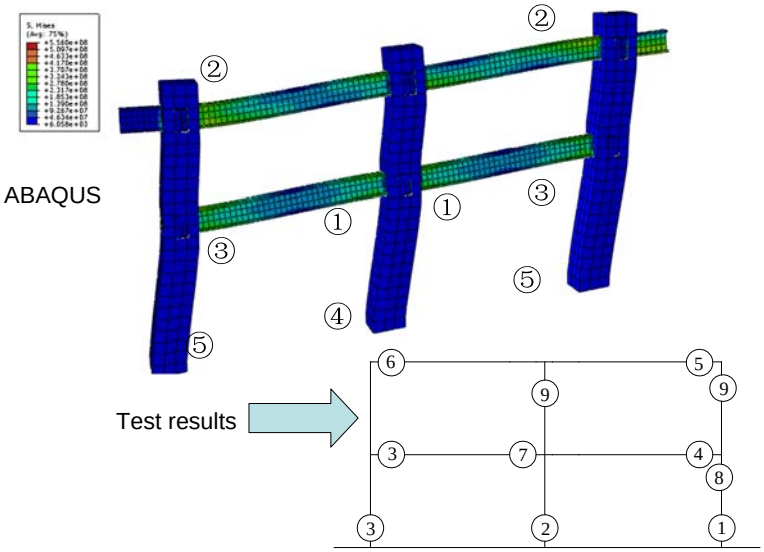

Figure 10. The order and location of plastic hinge that appeared in the RCS framed specimen.

DOI: 10.1002/tal

model developed in the previous section will be used to analyze composite CCSHECS frame structure; for comparison with the composite RCS frame structure, only the hoop strength and area are changed in the model parameters.

4.2. Development of model for composite CCSHRCS frame

In order to compare the composite CCSHRCS frame structure with the composite RCS frame structure, only the strength of the stirrups and area in the composite CCSHRCS frame model are changed, and the other parameters are the same as those of the composite RCS frame model of the previous section: to take yield strength of stirrups with 1000 MPa, to apply well-shaped compound spiral stirrups and to take uniform stirrups spacing with 50 mm to simplify the model. The model is shown in Figure 11.

4.3. The analysis of CCSHRC

Composite CCSHRCS frame under the effect of constant axial load for the top of the column and the horizontal loads for the beam end, composite CCSHRCS framed columns and framed beam belong to the bending components; therefore, the section of framed beam and column with horizontal load increases. The general law of framed column section changes is that from the whole cross-section compression when the horizontal load is zero, with the increase of horizontal load, tension zone begins to appear, and the neutral axis has been offset with the increasing horizontal load. On the section, the compression area becomes smaller and smaller, but the tension area is largely increasing. Therefore, to understand the mechanical properties of composite CCSHRCS frame easily, the composite CCSHRCS framed column for bending component is analyzed first.

To facilitate understanding of the stress state of concrete under different load steps, distribution of stress of concrete of CCSHRC is given under eight load steps as follows (and as shown in Figure 12).

Step 1. In the first load step, the axial load is applied only to the top of column, and the axial load for the interior column is as twice as that for the exterior column. In the figure, the vertical maximum compressive stress of concrete is 8.305 MPa, which is less than 26.9 MPa; therefore, it does not reach the compressive yield strength of concrete, so the concrete does not yield. The longitudinal stress for concrete of the interior column is significantly greater than that of both exterior columns.

Step 2. In the second load step, the axial load applied to the top of interior column in the first load step is maintained such that in later load steps, axial load applied to top of the column is transmitted and remains unchanged. At the same time, a displacement load of 0.01 m was applied to the beam end. At this moment, the maximum longitudinal compressive stress of concrete is 20.67 MPa, which is less than 26.9 MPa, so it has not yet reached the concrete compressive yield strength; this time, the longitudinal compressive stress of the concrete at the bottom of the interior column is maximal, followed by longitudinal compressive stress of concrete column joints and the bottom of the right column. The maximum longitudinal tension stress of concrete is 1.30 MPa, which has not yet reached yield.

Step 3. In the third load step, a displacement load of 0.04 m is applied to the beam end. The longitudinal compressive stress of concrete in the interior column joints has a maximum of 40.10 MPa, which is more

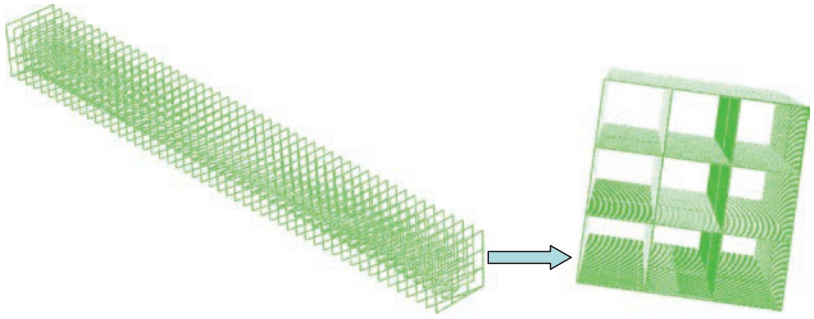

Figure 11. The finite element model of CCSH.

DOI: 10.1002/tal

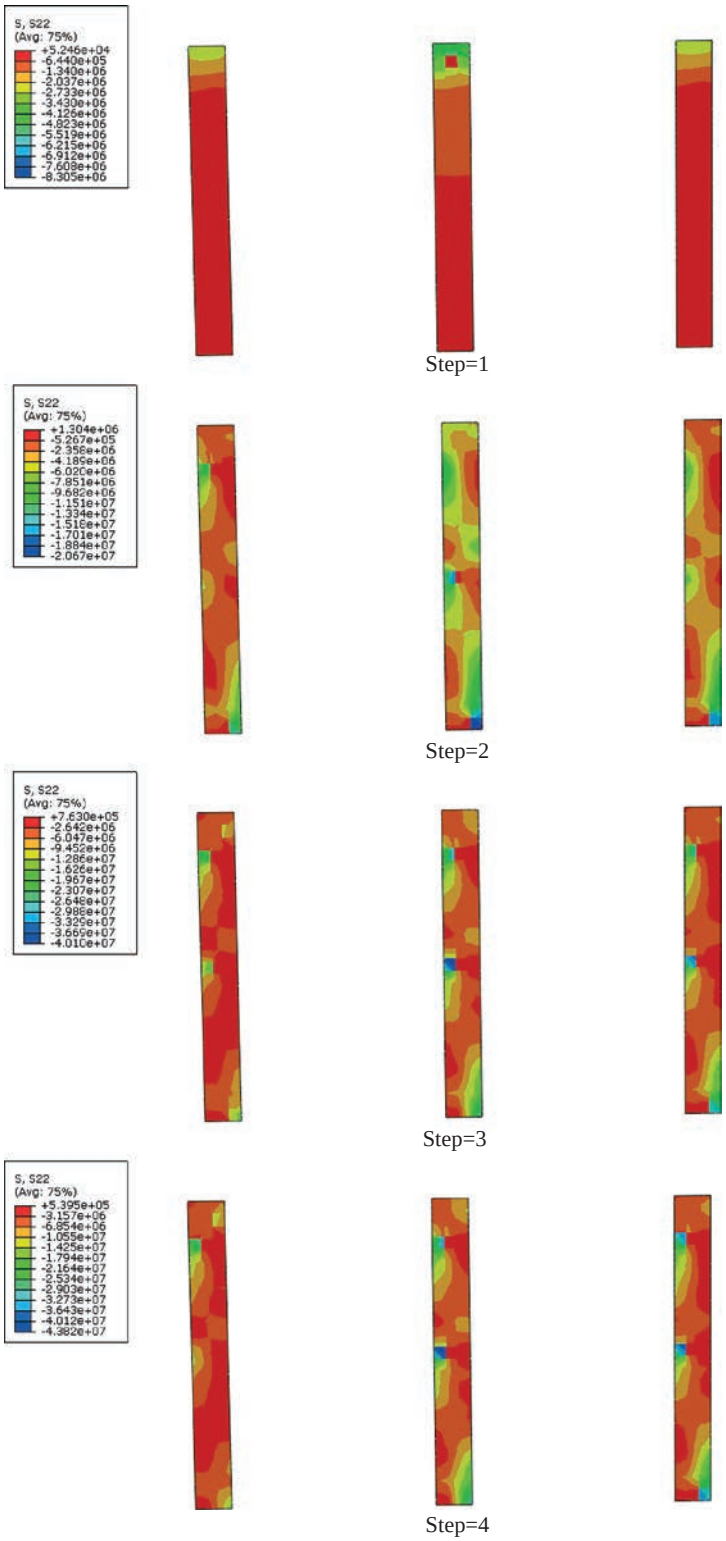

Figure 12. Distribution of stress of concrete of CCSHRC.

than the 26.9 MPa compressive yield strength of concrete. The longitudinal stresses of concrete of the right column at the bottom and the exterior joint area, which are 29.8 MPa and 33.28 MPa, are also greater than the compressive strength of concrete. Then, concrete begins to enter the cracking stage.

DOI: 10.1002/tal

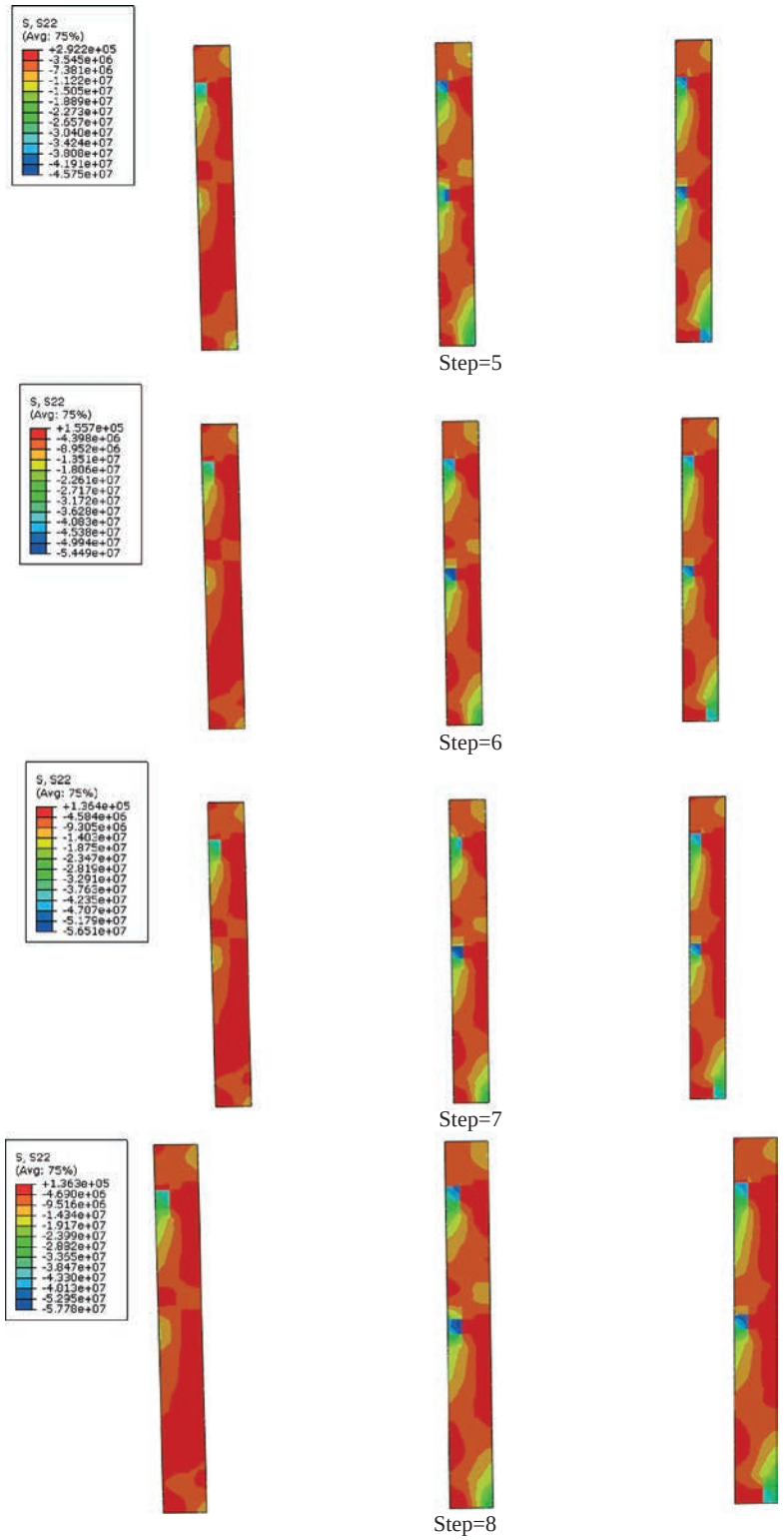

Figure 12. *(continued)*

Step 4. In the fourth load step, a displacement load of 0.06 m is applied to the beam end. At this time, the concrete in the interior column joints, in the bottom of the right column and in the exterior column joint area continues to develop cracks, whereas the longitudinal compressive stress of concrete at the

DOI: 10.1002/tal

top level of the interior column joint, in the bottom of the right column and at the top level of the right column is 32.72 MPa, which also exceeds the compressive strength of the concrete, and the concrete enters into the cracking stage.

Step 5. In the fifth load step, a displacement load of 0.08 m is applied to the beam end. At this time, the concrete in the middle and top levels of the interior column joints and exterior right column and in the top level of the right column joint enters into the stage working with cracks. The longitudinal compressive stress of concrete at the top of the left column is 30.40 MPa, exceeding the compressive strength of concrete, and concrete enters into the cracking stage.

Step 6. In the sixth load step, displacement load of 0.12 m is applied to the beam end. The yield of concrete area is the same as the fifth load step at this time, but the longitudinal compressive stress of concrete is much higher than the compressive strength of concrete at this time, in which crushing damage occurs for concrete.

Step 7. In the seventh load step, displacement load of 0.14 m is applied to the beam end. The yield of concrete area is the same as the sixth load step at this time. The yield part of concrete continues to produce some crushing damage, whereas concrete with longitudinal compressive stress of 32.91 MPa in the bottom of the interior column enters into the cracking stage.

Step 8. In the eighth load step, displacement load of 0.16 m is applied to the beam end. The yield of concrete area is the same as that of the sixth load step at this time. The yield part of concrete continues to produce some crushing damage. Compared with the seventh load step, the longitudinal compressive stress of concrete increases slowly at this time and compressive strain continues to increase, generating a large number of crushing damage in concrete.

4.4. The analysis of continuous compound spiral stirrups

Continuous compound spiral stirrups of composite CCSHRCS columns under load are under the effect of horizontal tension or compression. In the eighth load step, only a number of the stirrups yield, and very small number of the stirrups reach ultimate strength.

Figure 13 shows the transverse stress contour of CCSH in the last load step. The stirrup yield in the middle and top-level joint region of the interior column and the top-level joint region of the left and right column is more than 1000 MPa, and there are some stirrups that reach ultimate strength of

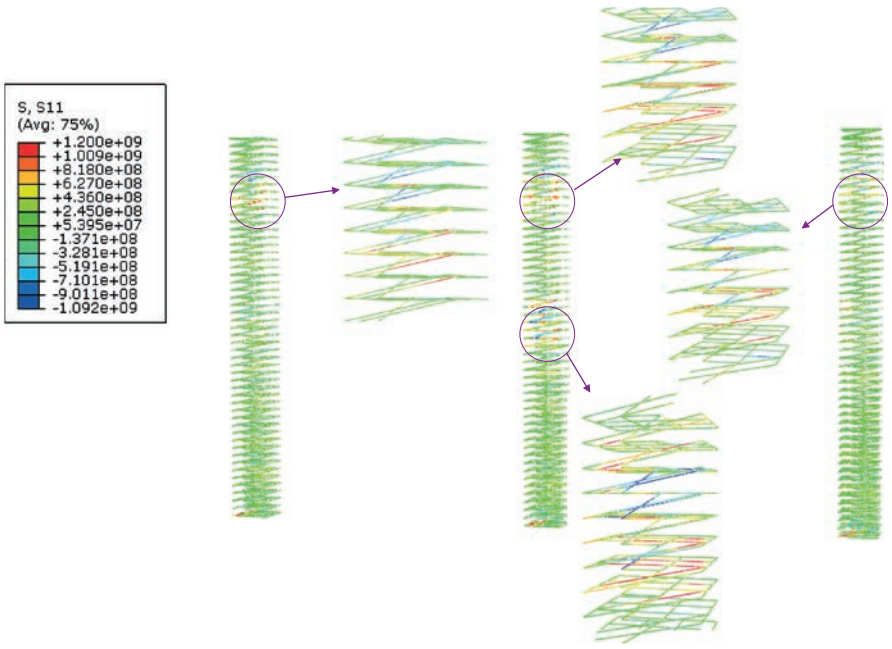

Figure 13. Distribution of lateral stress of CCSH (Step 8).

DOI: 10.1002/tal

1200 MPa. A small number of stirrups in the bottoms of three columns yield and reach ultimate strength. It indicates that the stirrups at both ends of the column are under a larger load, so they need to be changed in view of the operability of the construction. The spacing between stirrups should not be less than 50 mm, so higher-strength steel can be used as stirrups to improve the shear behavior of the components.

Since the concrete in the model in this paper is just an ordinary concrete, before the stirrups yield, the core concrete has long yielded and been destroyed but can still continue to bear. It is mainly because the high-strength stirrups are well confined with the core concrete, thus limiting the transverse strain development in core concrete and increasing the ultimate strength and deformation capacity of the column. Figure 14 confirms this point that in the last load step, due to the core concrete confined with the high-strength stirrups, the maximum transverse compressive strain of the core concrete is 0.0004209, and it is six times smaller than the average ultimate compressive strain of concrete.

4.5. The analysis of reinforcement

In the longitudinal reinforcements of composite CCSHRCS framed column under load, bonding exists between the concrete and the longitudinal reinforcements, and this interaction would expose the longitudinal reinforcements to tension or compression.

It is assumed that the concrete and the longitudinal reinforcements are fully bonded in the model. Figure 15 is the distribution of stress of reinforcement of the composite CCSHRCS framed columns under the final load step. The figure shows that almost all longitudinal reinforcements yield for the column, most of the longitudinal reinforcements at the bottom of the column reach the ultimate tension strength, the longitudinal reinforcements of the joint area have larger load and the tension stress in the longitudinal reinforcements generally is larger than the compressive stress. This is because monotonic loading was used in the model, and the horizontal displacement load is gradually increasing. Therefore, the tension stress in the longitudinal reinforcements is gradually increasing; the tension strength of the concrete is far below the compressive strength, so the concrete in the tension area withdraws from

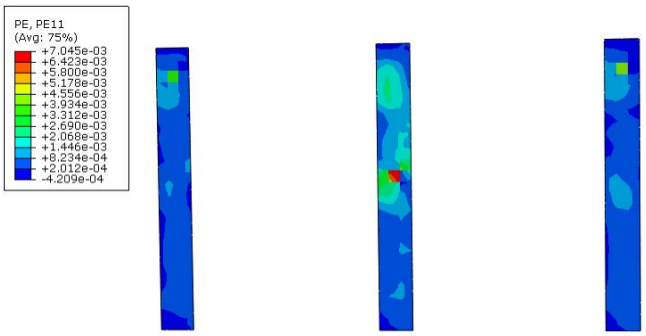

Figure 14. Distribution of lateral stress of concrete of CCSHRC (Step 8).

Figure 15. Distribution of stress of reinforcement of CCSHRC (Step 8).

DOI: 10.1002/tal

cracking and is destructed earlier. The tension stress entirely by the longitudinal reinforcement at this point is more than the compressive stress.

The elastic and plastic strain of the longitudinal reinforcements can also be observed. Figure 16 shows the distribution of elastic strain of reinforcements, and the elastic strain of the longitudinal reinforcements on the left of the column is greater than that on the right column. Figure 17 also shows the distribution of plastic strain of the reinforcements, and the plastic strain of the longitudinal reinforcements on the left of the column is also greater than that on the right column.

Under the same loading conditions, if raising the strength of the longitudinal reinforcements is bound to reduce the elastic and plastic strain of the longitudinal reinforcements, thus increasing the bearing capacity of the columns thereby increases the bearing capacity of the composite CCSHRCS frame. The premise above is that the stirrups have sufficient constraints on the core concrete columns, because even how high the strength of the longitudinal reinforcements is, if the stirrups lose constraints on the core concrete, it will result in the stirrups pulling off and the concrete to crack and be seriously damaged, leading the whole components to lose bearing capacity. Therefore, the good constraint of stirrups on the concrete of core area is prerequisite to improve the ultimate strength and deformation capacity of the components.

4.6. The analysis of steel beam and face bearing plate

The steel beam is adopted by the composite CCSHRCS framed beam, and its joint is a 'through-beam type'. The steel beam under the horizontal loads will deform and then yield occurs, and in order to understand the stress characteristics and the yield order of the steel beam end, the steel beam of joint region and the face bearing plate more clearly, Figure 18 shows the active yield flag at the integration points of the steel beam during the first and the eighth load step. The steel beams yield neither in the

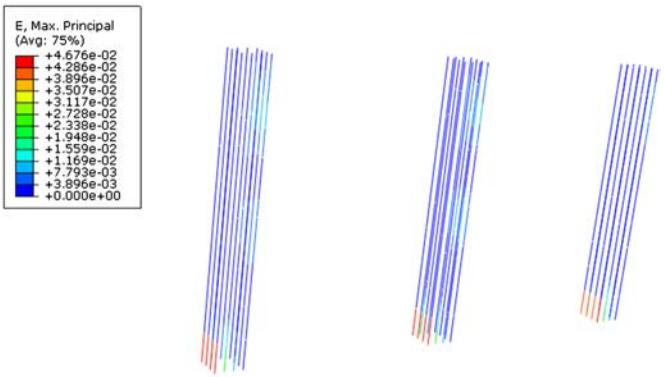

Figure 16. Distribution of elastic strain of reinforcement of CCSHRC (Step 8).

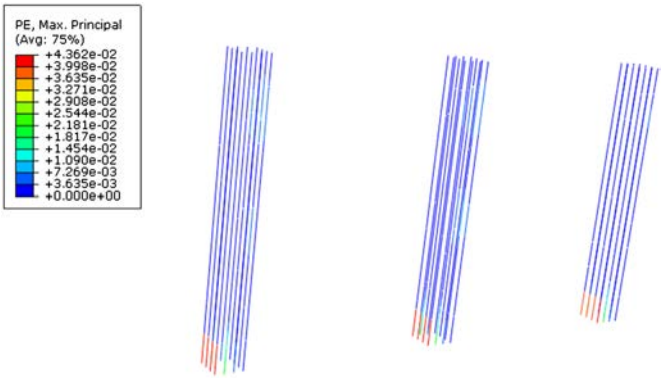

Figure 17. Distribution of plastic strain of reinforcement of CCSHRC (Step 8).

DOI: 10.1002/tal

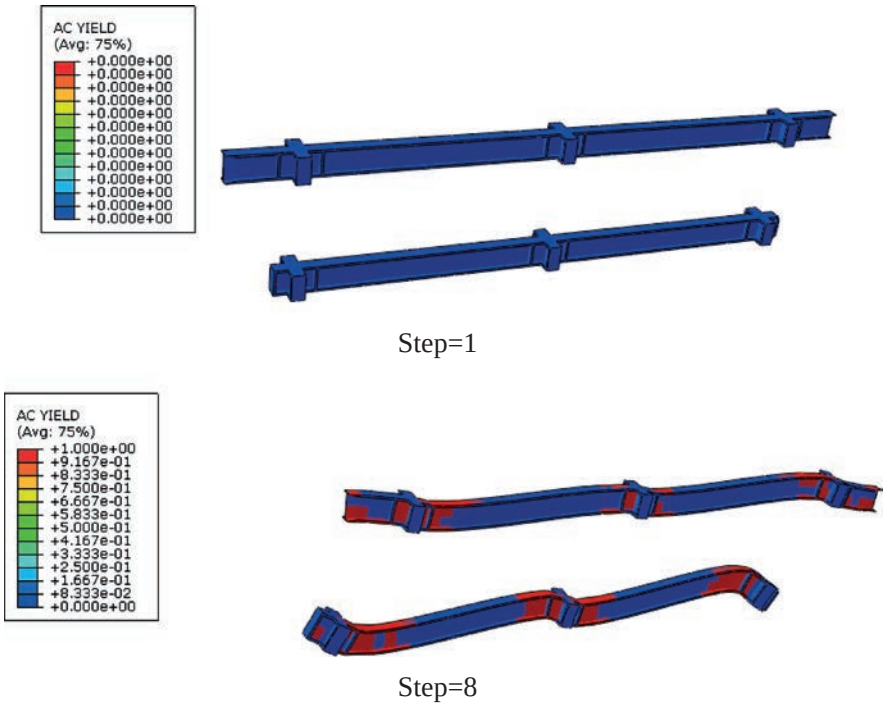

Figure 18. Active yield flag at integration points of steel beam during different steps of load.

first load step nor in the second load step. In the third load step, the second floor joint region, the steel beams of the second floor and beam end near the joint region appear to yield. Through the specific time point of concrete load step in the third load step, we can clearly distinguish the yield order of the steel beam. In the third load step, when the step time = 0.2223, the upper flange of the steel beams at the right column joint region on the second floor appears to yield first.

In the fifth load step, the plastic deformation of the upper flange on the beam end near the top joint region of the left and right column continues to develop, and the lower flange of the beam yields. In the sixth load step, the upper and lower flange of beam end near the top-level joint region in the interior column yields. At this time, the joint region and beam end have entered into the plastic yield phase.

In the eighth load step, plastic deformation of the steel beams continues to develop. The steel beam joint region and the beam end of the second floor reach the ultimate strength, and there is a greater warping on the beam end, as shown in Figure 19. Then, the beam end web and flange in the joint region of the left and right column and steel beams in interior column joint region begin to crack and break.

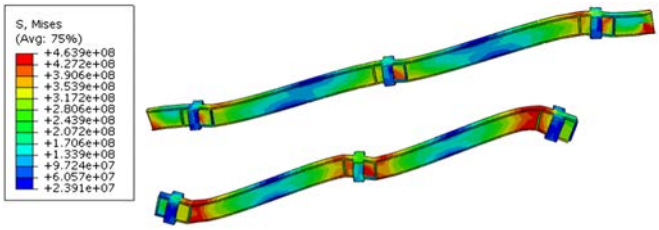

Figure 19. Mises stress of steel beam during the eighth step of load.

DOI: 10.1002/tal

4.7. The analysis of lateral load–displacement of composite CCSHRCS frame

The lateral load–displacement relationship of the composite CCSHRCS frame is obtained by numerical analysis, as shown in Figure 20. In the initial loading stages of the frame structure, horizontal displacement is within 15 mm, the structure has not yet reached the ultimate bearing capacity and the load–displacement curve approximate to a linear increasing relationship. After the horizontal displacement has exceeded 15 mm, loading is nonlinearly increasing, and the curve is smooth without the occurrences of obvious descent segment and inflection point in the load–displacement curve with the continuous increase of displacement. It is because the stirrups in the model are high-strength stirrups, which have better constraints on the concrete columns. Although a large number of cracks occur in the concrete, the concrete in the core area is firmly constrained by the high-strength stirrups, increasing the bearing and deformation capacity. This is very favorable in improving the anti-collapse performance of the structure under rare earthquake or extreme loads, but considering the yield failure that occurred in the concrete of the internal structure, according to the analysis results of the ABAQUS load steps, after the sixth load step, the columns and steel beams in the composite CCSHRCS frame a significant amount of yield failure that it reached the limit load of 968.04 kN and the corresponding horizontal displacement of 129.158 mm. Since the specimens of the model and those in the literature (Iizuka *et al*., 1997; Li *et al*., 2011) are in the same size, different material parameters are the same in addition to the stirrups, and the ultimate lateral bearing and horizontal displacements have increased by 9.38% and 29%, respectively, compared with the test values in the literature. This further indicates that high-strength stirrups can improve the bearing and deformation capacity of a composite CCSHRCS frame.

5. SUMMARY AND CONCLUDING REMARKS

In this paper, the mechanical behaviors of a composite frame (CCSHRCS) consisting of continuous compound spiral hoop reinforced concrete (CCSHRC) column and steel (S) beam are simulated by using finite element software ABAQUS, which describes the basic principles of the concrete plastic-damage model. First, a dimensional nonlinear finite element model of RCS frame specimens that tested in the literature by using the ABAQUS software is developed, and this model is validated by using the horizontal load–horizontal displacement relationship, story drift ratio and failure modes of RCS frame structures in the experimental data. Model results agree well with the test results, and then the model was used for further preliminary analysis of the composite CCSHRCS frame, only changing the strength of the stirrups and stirrup form in the model. The results have shown that continuous compound spiral high-strength stirrups could effectively improve the lateral deformation capacity of

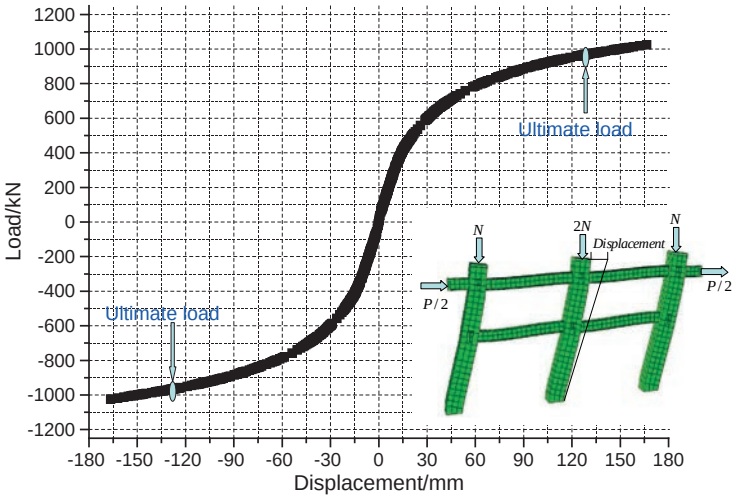

Figure 20. Relationship of load–displacement of composite CCSHRCS frame.

DOI: 10.1002/tal

concrete, with a good constraint to the concrete in the core area under the same load conditions, thereby increasing the ultimate lateral bearing and deformation capacity of the composite CCSHRCS frame. When high-strength stirrups are under the load, only a small number of stirrups at the bottom of the column and the joint region yield, and very few stirrups reach the ultimate strength. This indicates that the stirrups under the ultimate load is well constrained to the core concrete. In addition, the strength of the longitudinal reinforcements has a significant impact on the composite CCSHRCS frame under the premise that the stirrups are well constrained in the core area of the concrete. With the strength of longitudinal reinforcements increasing; the horizontal load and deformation capacity of the frame will increase. The yield order of the steel beam and the face bearing plate is obtained under different load steps by calculation, providing a reference for the detailed structural design of components. Finally, the horizontal load–displacement curve of the composite CCSHRCS frame is analyzed. As high-strength stirrups has good constraints on the core concrete, most of the concrete, steel beams and face bearing plates have reached the stage of yield failure, but the load is capable of increasing, indicating that the high-strength stirrups can improve the anti-collapse capacity of the composite CCSHRCS frame. According to the analysis results of the ABAQUS load steps, after the sixth load step is completed, many columns and steel beams in the composite CCSHRCS frame have reached yield failure, with an ultimate load of 968.04 kN and corresponding horizontal displacement of 129.158 mm. In this condition, the ultimate lateral bearing and horizontal displacement increased by 9.38% and 29%, respectively, compared with those tested in the literature. This further indicates that high-strength stirrups can improve the horizontal bearing and deformation capacity of a composite CCSHRCS frame structure.

ACKNOWLEDGEMENTS

The authors would like to express appreciation to the Xi'an University of Architecture & Technology and colleagues. We also thank the Architectural Institute of Japan for providing the beneficial materials.

The writers would like to acknowledge the contributions by many investigators from Japan and the USA. Many of whom are identified through the referenced papers and reports.

REFERENCES

ABAQUS User's Manual—Version 6.8.1. Hibbit, Karlsson & Sorenson, Pawtucket, RI, 2006.

Bursi OS, Sun FF., Postal S. 2005. Non-linear analysis of steel–concrete composite frames with full and partial shear connection subjected to seismic loads. *Journal of Constructional Steel Research* **61**: 67–92.

Carol I, Prat PC, Bazant ZP. 1992. New explicit microplane model for concrete: theoretical aspects and numerical implementation. *International Journal of Solids and Structures* **29**(9): 1173–1191.

Goel SC. 2004. United States–Japan Cooperative Earthquake Engineering Research Program on Composite and Hybrid Structures. *Journal of Structural Engineering, ASCE* **130**(2): 157–158.

Hajjar J, Leon R, Gustafson M, Shield C. 1998. Seismic response of composite moment-resisting connections. II: behavior. *Journal of Structural Engineering, ASCE* **124**(8): 877–885.

Han LH, Wang WD, Zhao XL. 2008. Behavior of steel beam to concrete-filled SHS column frames: finite element model and verifications. *Engineering Structures* **30**: 1647–1658.

Hu HT, Huang CS, Wu MH, Wu YM. 2003. Nonlinear analysis of axially loaded concrete-filled tube columns with confinement effect. *Journal of Structural Engineering, ASCE* **129**(10): 1322–1329.

Iizuka S, Kasamatsu T, Noguchi H. 1997. Study on the seismic performances of mixed frame structures. *Journal of Structure and Construction Engineering of Architecture Institute of Japan* **497**: 189–196 [in Japanese].

Li W, Li QN, Jiang WS, Jiang L. 2011. Seismic performance of composite reinforced concrete and steel moment frame structures state-of-the-art. *Composites: Part B* **42**(2): 190–206.

Liu J, Foster SJ. 1998. Finite element model for confined concrete columns. *Journal of Structural Engineering, ASCE* **124**(9): 1011–1017.

Salvatore W, Bursi OS, Lucchesi D. 2005. Design, testing and analysis of high ductile partial-strength steel-concrete composite beam-to-column joints. *Computers and Structures* **83**: 2334–2352.

Wu LY, Chung LL, Wang MT, Huang GL. 2009. Numerical study on seismic behavior of H-beams with wing plates for bolted beam–column connections. *Journal of Constructional Steel Research* **65**: 97–115.

Yu T, Teng JG, Wong YL, Dong SL. 2010a. Finite element modeling of confined concrete—I: Drucker–Prager type plasticity model. *Engineering Structures* **32**: 665–679.

Zhao GZ, Li A. 2008. Numerical study of a bonded steel and concrete composite beam. *Computers and Structures* **86**: 1830–1838.

DOI: 10.1002/tal

AUTHORS' BIOGRAPHIES

Wei Li was born in 1981. He is a native of Wannian, Jiangxi Province, China. He graduated with honors from Nanchang University in 2005 with a BS in Civil Engineering. Subsequently, he attended Nanchang University to pursue an MS in Civil/Structural Engineering Department in 2005. After receiving an MS in Structural Engineering in 2008, he attended the Xi'an University of Architecture and Technology to pursue a PhD in Civil/Modern Structural Theory in 2008. After receiving his PhD degree from Xi'an University of Architecture and Technology in Nov. 2011, he joined the faculty of Civil Engineering Department at Wenzhou University as a lecturer. His research interests refer to a variety of topics. They include seismic performance study on composite frames consisting of reinforced concrete column and composite beam as well as shear wall structures. He also explored a number of other research areas, including performance-based seismic design of steel and concrete structures as well as damage assessment of structures.

Qing-ning Li received his Bachelor's degree in Civil Engineering from the Xi'an University of Architecture and Technology, Xian, China, in June 1974. He is now a professor in the Department of Civil Engineering in the Xi'an University of Architecture and Technology. He is interested in the area of numerical analysis of bridge structures as well as steel and concrete structures.

Wei-shan Jiang received his Bachelor's degree in Civil Engineering from Northeast University, Shenyang, China, in June 1951. He is now a professor in the Department of Civil Engineering in the Xi'an University of Architecture and Technology. His research interests focus on design and behavior of reinforced and pre-stressed concrete, composite, or hybrid structures.

DOI: 10.1002/tal